Closed-Loop Adaptive Switched-Capacitor Step-Down DC-DC Converter for Piezoelectric Energy Harvesting

Yuen-Haw Chang and Chun-Hung Wang

***Abstract*—A closed-loop scheme of adaptive switched-capacitor converter (ASCC) is presented by combining a phase generator and non-overlapping circuit to realize the switched-capacitor-based (SC) step-down conversion for piezoelectric energy harvesting. In the power part of ASCC, there are two cascaded sub-circuits including: (i) Front: the bridge rectifier and a filter capacitor (C_i), and (ii) Core: 5-stage serial-parallel SC step-down converter and an output capacitor (C_o). By using the front bridge rectifier, it converters the AC source of piezoelectric device into the DC source, and then harvests the energy to store in the filter capacitor C_i for building the DC supply V_s. The core 5-stage serial-parallel SC converter can provide 5 different step-down voltages ($\frac{V_s}{5}, \frac{V_s}{4}, \frac{V_s}{3}, \frac{V_s}{2}, V_s$), and with the help of the phase generator, perform an adaptive charging operation stage by stage (from the lower voltage to the higher one) for the protection of the battery load. Finally, the closed-loop ASCC is designed by OrCAD Pspice, and simulated for some cases: steady-state and dynamic responses (source/loading variation). All results are illustrated to show the efficacy of the proposed scheme.**

***Index Terms*—adaptive, piezoelectric, harvesting, switched-capacitor, step-down converter, serial-parallel.**

I. Introduction

Recently, with the rapid development of power electronics technology, the demand on voltage supply increases more and more. The step-up/down DC-DC converters are employed more widely for the electricity -supply applications, such as photovoltaic system (PV), fuel cell, X-ray systems, and are asked for some characteristics of light weight, small volume, high efficiency and better regulation capability.

The SC power converter based on structure of charge pump is one of the good solutions to low power and high gain DC-DC conversion, because it has only semiconductor switches and capacitors. Unlike traditional converters, SC converter needs no magnetic element, so it has light weight and small volume and low EMI. However, most SC circuits have voltage gain proportional to the number of pumping capacitors. Now, various SC types have been suggested and the well-known topologies are described as follow. In 1976, Dickson charge pumping was proposed based on a diode-chain structure via pumping capacitors [1]. It provides voltage gain proportional to the stage number of pumping capacitor, and the detailed dynamic model and efficiency analysis were discussed [2]. But, its drawbacks include the fixed voltage gain and the larger device area. In 1993, Ioinovici *et al.* suggested a voltage-mode SC with two symmetrical capacitor cells working complementarily [3]. In 1997, Zhu and Ioinovici performed a comprehensive steady-state analysis of SC [4]. In 2009, Tan *et al.* proposed a low-EMI SC by interleaving control [5]. In 2011, Chang proposed an integrated SC step-up/down DC-DC/DC-AC converter/inverter [6]-[8]. In 2002, Ottman *et al.* proposed the prototype of piezoelectric energy harvesting circuit based on the LC resonant booster for wireless remote power supply [9]. In this paper, with on magnetic elements, the closed-loop adaptive SC-based piezoelectric energy harvesting circuit is presented to achieve the multistage charging operation of battery.

Manuscript received December 5, 2013. This work is supported in part by the National Science Council of Taiwan, R.O.C., under Grant NSC 102-2221-E-324-030.

Yuen-Haw Chang and Chun-Hung Wang are with the Department and Graduate Institute of Computer Science and Information Engineering, ChaoYang University of Technology, Taichung, Taiwan, R.O.C. Post code: 413. (e-mail: cyhfyc@cyut.edu.tw, s10127609@gm.cyut.edu.tw).

II. Configuration of ASCC

Fig. 1 shows the overall circuit configuration of closed-loop ASCC, and it contians two major parts: power part and control part for an adaptive multi-stage charging operation of battery. Fig. 2 shows the detailed logic circuit of the control part.

A. Power part

The power part of ASCC is shown in the upper half of Fig. 1, and it consists of a bridge rectifier and SC step-down DC-DC converter connected in series between the piezoelectric device and the battery load. The bridge rectifier contains 4 diodes (D_1-D_4) and one input filter capacitor C_i to obatin a rectified, filtered, and stable supply voltage V_s. The SC step-down converter is composed of 5 pumping capacitors (C_1-C_5), 7 power switches (S_1-S_5, S_i, S_o), one ouput filiter capacitor C_o, and 8 diodes (D_5-D_{12}), where each capacitor has the capacitance C (C_1=C_2=C_3=C_4=C_5=C). Fig. 3 shows the theoretical waveforms of ASCC. Here, the whole charging operation is scheduled and divided into 5 stages (Stage I, II, III, IV, and V) for the protection of the battery load, especially for the lower battery voltage. In each stage, there are two interleaved operations: charging capacitors in series (as ϕ_1=1) and discharging capacitors in parallel (as ϕ_2=1), where ϕ_1 and ϕ_2 are a set of non-overlapping anti-phase signals, so as to realize the SC step-down conversion. The operations of these 5 stages are described as follows.

(i) Stage I : between 0 and $\frac{V_s}{5}$

At the charging cycle (ϕ_1=1), turn on S_i, S_5, and

ISBN: 978-988-19253-3-6
ISSN: 2078-0958 (Print); ISSN: 2078-0966 (Online)

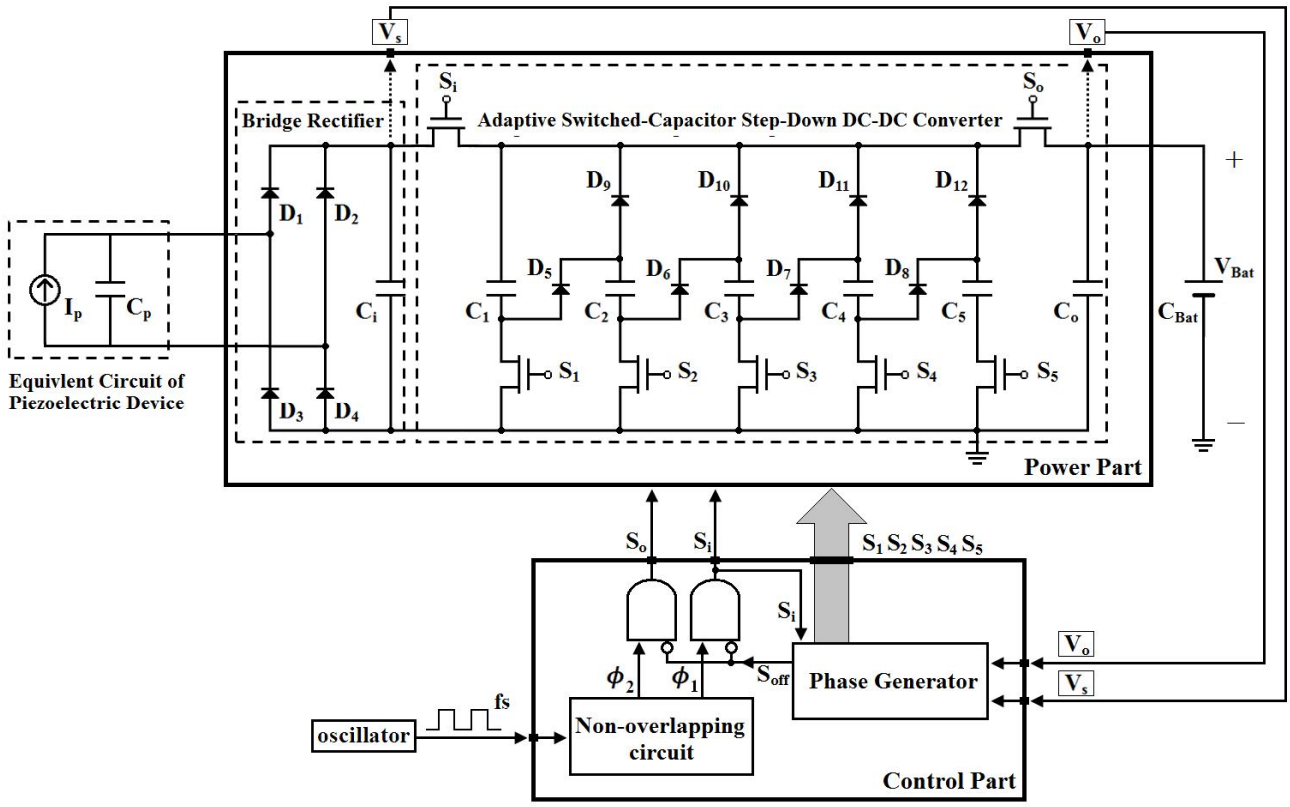

Fig. 1. Configuration of closed-loop ASCC.

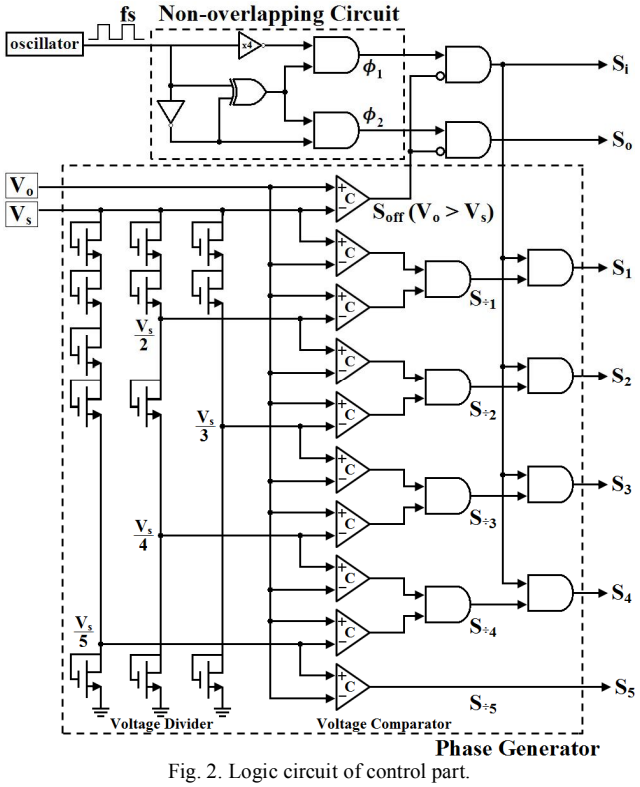

Fig. 2. Logic circuit of control part.

turn off S_o, S_1-S_4. Then, the diodes D_5-D_8 are on, and D_9-D_{12} are off. The current-flow path is shown as "—" in Fig. 4(a). The capacitors C_1-C_5 are charged in series by source V_s. At the discharging cycle (ϕ_2=1), C_1-C_5 are discharged in parallel to supply the energy to output filter capacitor C_o and battery load C_{Bat}. The current-flow path is shown as "---" in Fig. 4(a).

(ii) Stage II : between $\frac{V_s}{5}$ and $\frac{V_s}{4}$

At the charging cycle (ϕ_1=1), turn on S_i, S_4, and turn off S_o, S_1-S_3, S_5. Then, the diodes D_5-D_7 are on, and D_8-D_{12} are off. The current-flow path is shown as "—" in Fig. 4(b). The capacitors C_1-C_4 are charged in series by source V_s. At the discharging cycle (ϕ_2=1), C_1-C_4 are discharged in parallel to supply the energy to output filter capacitor C_o and battery load C_{Bat}. The current-flow path is shown as "---" in Fig. 4(b).

(iii) Stage III : between $\frac{V_s}{4}$ and $\frac{V_s}{3}$

At the charging cycle (ϕ_1=1), turn on S_i, S_3, and turn off S_o, S_1, S_2, S_4, S_5. Then, the diodes D_5, D_6 are on, and D_7-D_{12} are off. The current-flow path is shown as "—" in Fig. 4(c). The capacitors C_1-C_3 are charged in series by source V_s. At the discharging cycle (ϕ_2=1), C_1-C_3 are discharged in parallel to supply the energy to output filter capacitor C_o and battery load C_{Bat}. The current-flow path is shown as "---" in Fig. 4(c).

(iv) Stage IV : between $\frac{V_s}{3}$ and $\frac{V_s}{2}$

At the charging cycle (ϕ_1=1), turn on S_i, S_2, and turn off S_o, S_1, S_3-S_5. Then, the diodes D_5 are on, and D_6-D_{12} are off. The current-flow path is shown as "—" in Fig. 4(d). The capacitors C_1, C_2 are charged in series by source V_s. At the discharging cycle (ϕ_2=1), C_1-C_2 are discharged in parallel to supply the energy to output filter capacitor C_o and battery load C_{Bat}. The current-flow path is shown as "---" in Fig. 4(d).

(v) Stage V : between $\frac{V_s}{2}$ and V_s

At the charging cycle (ϕ_1=1), turn on S_i, S_1, and

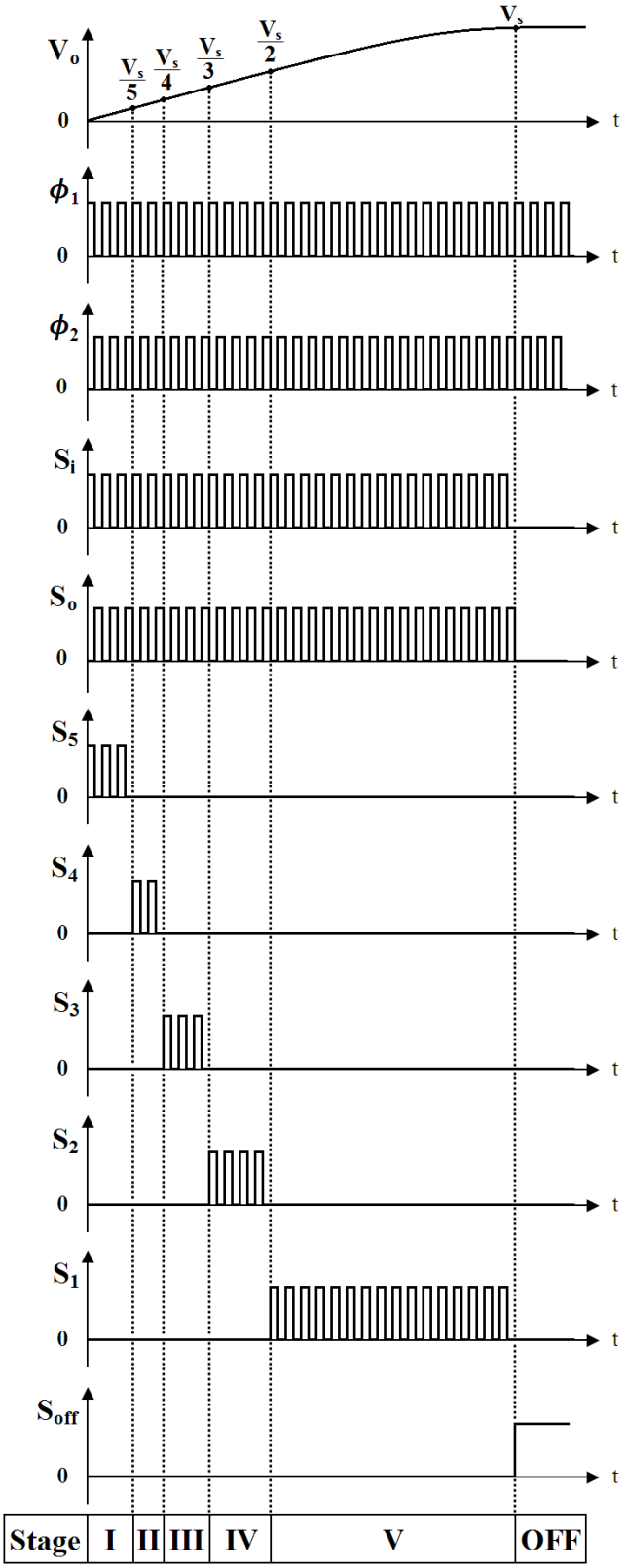

Fig. 3. Theoretical waveforms of ASCC.

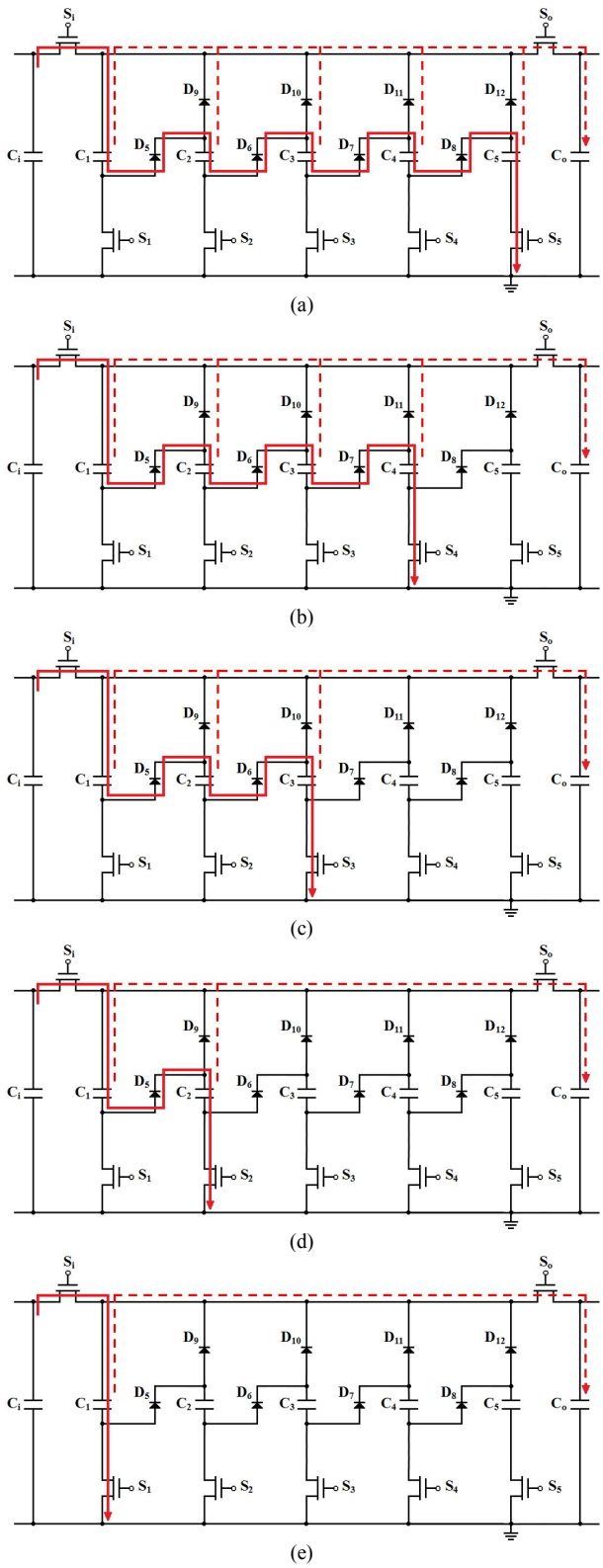

Fig. 4. Topologies for stage (a)I, (b)II, (c)III, (d)IV, and (e)V.
("—" : charging cycle as ϕ_1=1, "---" : discharging cycle as ϕ_2=1)

turn off S_o, S_2-S_5. Then, the diodes D_5-D_{12} are off. The current-flow path is shown as "—" in Fig. 4(e). The capacitors C_1 are charged in series by source V_s. At the discharging cycle (ϕ_2=1), C_1 are discharged in parallel to supply the energy to output filter capacitor C_o and battery load C_{Bat}. The current-flow path is shown as "---" in Fig. 4(e).

Based on the operations as above, the battery voltage V_{Bat} can be raising up to the supply voltage V_s stage by stage. This way can avoid large peak current on the battery to extend the usage lifetime of battery.

B. Control part

The control part of ASCC is shown in the lower half of Fig. 1, and its detailed logic circuit is as in Fig. 2. It is

ISBN: 978-988-19253-3-6
ISSN: 2078-0958 (Print); ISSN: 2078-0966 (Online)

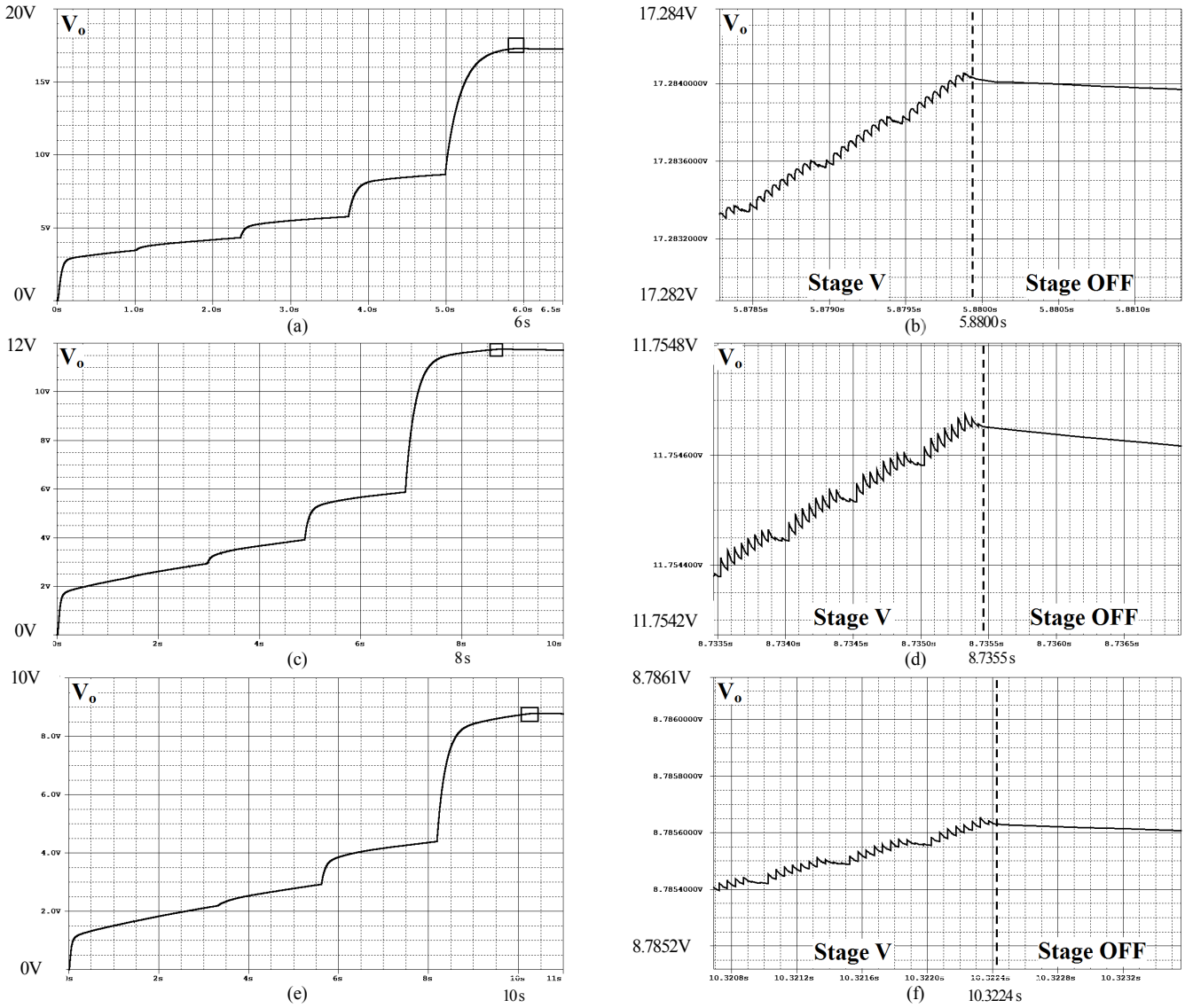

Fig. 5. Steady-state response of ASCC for Case I : (a)(b) V_s = 18V, Case II : (c)(d) V_s = 12V, and Case III : (e)(f) V_s = 9V.

composed of non-overlapping circuit and phase generator. From the controller signal flow, the feedback signals V_o and V_s are sent into the phase generator for making the switch signals S_1-S_5. In the phase generator, it includes the NMOS-based voltage divider, voltage comparator, and some AND logic gates. This voltage divider has a NMOS-cascaded structure to produce a various division of supply voltage V_s as : $\frac{V_s}{5}$, $\frac{V_s}{4}$, $\frac{V_s}{3}$, $\frac{V_s}{2}$, and V_s. In the voltage comparator, the output voltage V_o is compared with these divisions of V_s in order to produce the basic control signals $S_{\div 1}$, $S_{\div 2}$, $S_{\div 3}$, $S_{\div 4}$, $S_{\div 5}$, S_{OFF} for the multi-stage operation. Finally, the practical switch signals S_1-S_5 can be obtained with the help of the synchronous operation of S_i via some AND logic gates. Here, S_i is the switch signal generated by ϕ_1 and S_{OFF} to control the energy transferring from the piezoelectric device to the SC bank, and S_o is generated by ϕ_2 and S_{OFF} to control the energy transferring from the SC bank to the battery load, where ϕ_1 and ϕ_2 are a set of non-overlapping clocks produced by the non-overlapping circuit. Based on these designs, the control part can generate these switch signals exactly like the waveforms in Fig. 3 for achieving the charging operation of battery stage by stage.

TABLE I
Components of ASCC

Rectified supply source (V_s)	18V
Pumping capacitor (C_1~C_5)	500nF
Filter capacitor (C_i, C_o)	500uF
Battery Capacitor (C_{Bat})	1mF
Power MOSFETs (S_i, S_o, S_1~S_5)	Mbreak N
Switching frequency (fs)	20kHz
Diodes (D_1~D_{12})	D1N5822

III. EXAMPLES OF ASCC

In this section, based on Fig. 1, the ASCC is designed and simulated by OrCAD Pspice tool. The results are illustrated to verify the efficacy of the proposed converter. The relevant component parameters are listed in Table I. For checking closed-loop performances, some topics will be discussed as including: (i) Steady-state response (ii) Dynamic response (source/loading variation).

(i) Steady-state response:

Case I:

Assume the supply voltage V_s is 18V, and then the steady-state result of output voltage V_o (within 6.5 sec) is obtained as in Fig. 5(a). Obviously, V_o is raising to get close to V_s = 18V stage by stage. After 5.88 sec, the

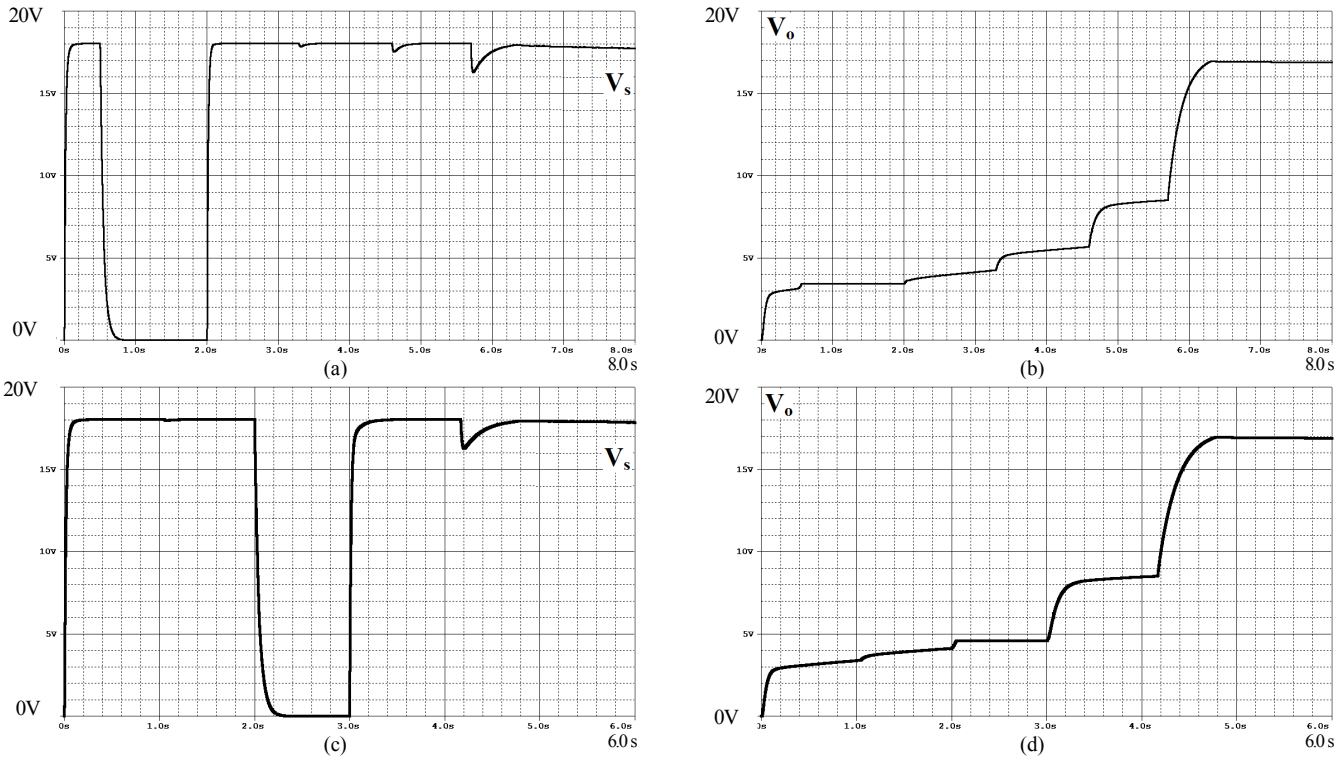

Fig. 6. Dynamic response of ASCC for source variation.
Case I : (a)(b) V_s = 18V→0V at 0.5sec, 0V→18V at 2.0sec. Case II : (c)(d) V_s = 18V→0V at 2.0sec, 0V→18V at 3.0sec

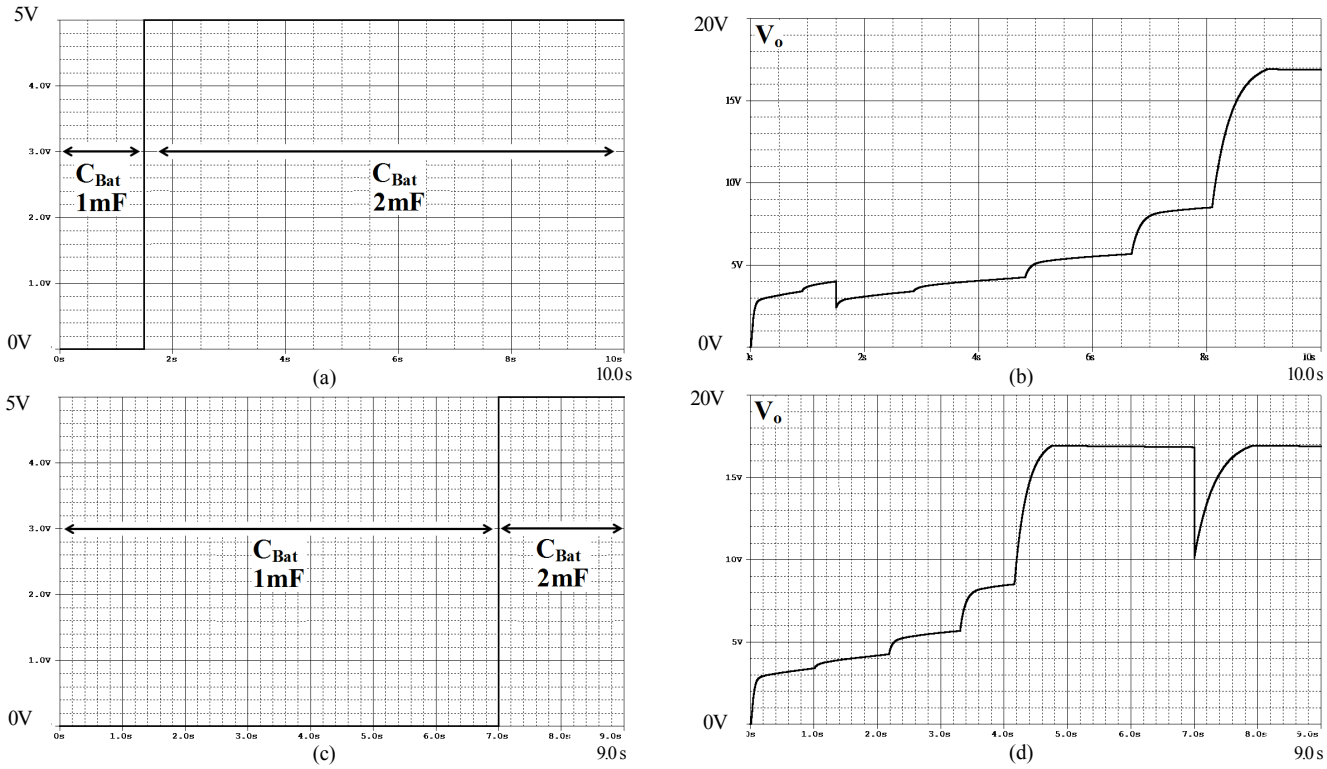

Fig. 7. Dynamic response of ASCC for loading variation.
Case III : (a)(b) C_{Bat} = 1mF → 2mF at 1.5sec. Case IV : (c)(d) C_{Bat} = 1mF → 2mF at 7.0sec

operation starts entering the Stage OFF as shown in Fig. 5(b). Now, the charged battery keeps its voltage at about 17.28V.

Case II:

Assume the supply voltage V_s is 12V, and then the steady-state result of output voltage V_o (within 10 sec) is obtained as in Fig. 5(c). Obviously, V_o is raising to get close to V_s = 12V stage by stage. After 8.73 sec, the operation starts entering the Stage OFF as shown in Fig. 5(d). Now, the charged battery keeps its voltage at about 11.75V.

Case III:

Assume the supply voltage V_s is 9V, and then the steady-state result of output voltage V_o (within 11 sec) is obtained as in Fig. 5(e). Obviously, V_o is raising to get close to V_s = 9V stage by stage. After 10.32 sec, the operation

ISBN: 978-988-19253-3-6
ISSN: 2078-0958 (Print); ISSN: 2078-0966 (Online)

starts entering the Stage OFF as shown in Fig. 5(f). Now, the charged battery keeps its voltage at about 8.78V.

(ii) Dynamic response:

Since the piezoelectric device always generates the kind of pulsing source voltage, it is not easy to provide a pure and constant supply. Also, the number/capacitance of battery could be changed. Thus, these two situations (source variation/loading variation) should be considered here.

Case I:

Assume that supply voltage V_s is 18V, and it has a voltage drop down to 0V from 0.5 sec to 2 sec as in Fig. 6(a). Fig. 6(b) shows the whole waveform of V_o. Obviously, the voltage level of V_o stops raising to hold at 3.4V during the interval of V_s = 0V. When V_s recovers back to 18V, V_o keeps going back to the charging operation.

Case II:

Assume that supply voltage V_s is 18V, and it has a voltage drop down to 0V from 2 sec to 3 sec as in Fig. 6(c). Fig. 6(d) shows the whole waveform of V_o. Obviously, the voltage level of V_o stops raising to hold at 4.6V during the interval of V_s = 0V. When V_s recovers back to 18V, V_o keeps going back to the charging operation.

Case III:

Assume that C_{Bat} is 1mF normally, and it changes from 1mF to 2mF at 1.5 sec as in Fig 7(a). Fig 7(b) shows the result of V_o. Clearly, it is found that V_o has a sudden voltage drop while C_{Bat}: 1mF→2mF. At the same time, the charging operation is going from Stage II back to Stage I for adapting the loading variation.

Case IV:

Assume that C_{Bat} is 1mF normally, and it changes from 1mF to 2mF at 7 sec as in Fig 7(c). Fig 7(d) shows the result of V_o. Clearly, it is found that V_o has a sudden voltage drop while C_{Bat}: 1mF→2mF. At the same time, the charging operation is going from Stage OFF back to Stage V for adapting the loading variation.

The above results show that the closed-loop ASCC has a good output regulation capability to source/loading variations.

IV. Conclusions

A closed-loop scheme of ASCC is presented by combining a phase generator and non-overlapping circuit to realize step-down conversion and regulation for piezoelectric energy harvesting. The advantages of the proposed scheme are listed as follows. (i) In the ASCC, there are totally 5 stages scheduled for running the charging operation in order to protect the battery load. (ii) The ASCC belongs to the kind of SC circuit, so it needs no magnetic element (like inductor or transformer). Thus, the fabrication of ASCC is promising in the future. (iii) In the control part, the adaptive phase generator with changing the

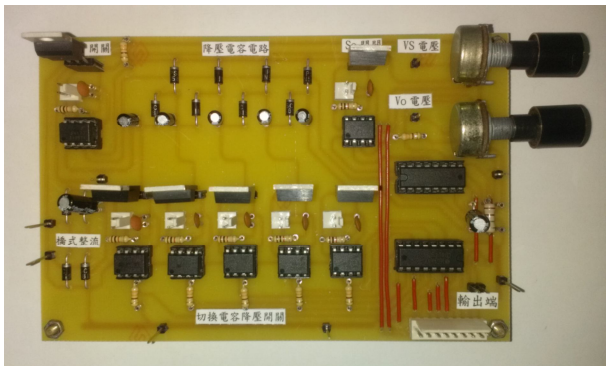

(a)

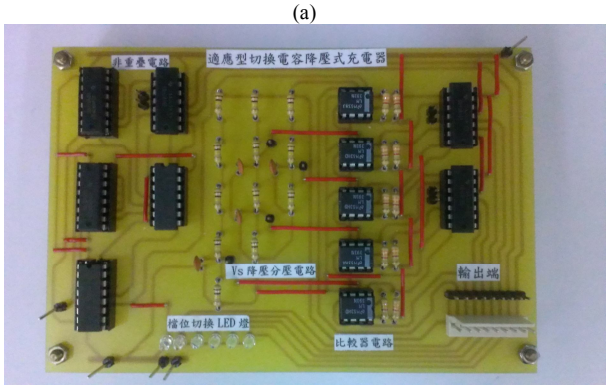

(b)

Fig. 8. Prototype circuit of closed-loop ASCC.
(a) power part (b) control part.

stage number is designed for being able to adapt the source/loading variations. At present, the prototype circuit of the proposed converter is implemented in the laboratory as shown the photo in Fig 8. Some experimental results will be obtained and measured for the verification of the proposed converter.

References

[1] J. K. Dickson, "On-chip high-voltage generation in MNOS integrated circuits using an improved voltage multiplier technique," *IEEE J. Solid-State Circuit,* vol. SC:-11, pp. 374-378, Feb. 1976.

[2] T. Tanzawa, and T. Tanaka. "A dynamic analysis of the Dickson charge pump circuit," *IEEE J. Solid-State Circuit,* vol. 32, pp. 1231-1240, Aug. 1997.

[3] S. V. Cheong, S. H. Chung, and A. Ioinovici, "Duty-cycle control boosts DC-DC converters," *IEEE Circuits and Devices Mag,* vol 9, no. 2, pp. 36-37, 1993.

[4] G. Zhu and A. Ioinovici, "Steady-state characteristics of switched-capacitor electronic converters," *J. Circuits, Syst. Comput.* , vol. 7, no. 2, pp. 69-91, 1997.

[5] S. C. Tan, M. Nur, S. Kiratipongvoot, S. Bronstein, Y. M. Lai, C. K. Tse, and A. Ioinovici, "Switched-capacitor converter configuration with low EMI obtained by interleaving and its large-signal modeling" *in Proc. IEEE Int. Symp. Circuits Syst.* pp. 1081-1084, May 2009.

[6] Y. H. Chang, "Variable conversion ratio multistage switched-capacitor voltage-multiplier/divider DC-DC converter," *IEEE Trans. Circuits Syst. I, Reg. Papers,* vol. 58, no. 8, pp. 1944-1957, Aug. 2011.

[7] Y. H. Chang, "Design and analysis of multistage multiphase switched-capacitor boost DC-AC inverter," *IEEE Trans. Circuits Syst. I, Reg. Papers,* vol. 58, no. 1, pp. 205-218, Jan. 2011.

[8] Y. H. Chang, "A Gain/Efficiency-Improved Serial-Parallel Switched-Capacitor Step-Up DC–DC Converter," *IEEE Trans. Circuits Syst. I, Reg. Papers,* vol. 60, no. 10, pp. 2799-2809, Oct. 2013.

[9] G. K. Ottman, H. F. Hofmann, A. C. Bhatt, and G. A. Lesieutre, "Adaptive Piezoelectric Energy Harvesting Circuit for Wireless Remote Power Supply," *IEEE Trans. on Power Electroics.,* vol 7, no. 5, pp. 669-676, 2002.

ISBN: 978-988-19253-3-6
ISSN: 2078-0958 (Print); ISSN: 2078-0966 (Online)